Journal of Molecular Graphics and Modelling 27 (2008) 394–400

Contents lists available at ScienceDirect

Journal of Molecular Graphics and Modelling

journal homepage: www.elsevier.com/locate/JMGM

Quantum chemical study of the intermediate complex required for iron-mediated reactivity and antimalarial activity of dispiro-1,2,4-trioxolanes

Darren J. Creek, David K. Chalmers *, William N. Charman, Brian J. Duke

Monash Institute of Pharmaceutical Sciences, Monash University (Parkville Campus), 381 Royal Parade, Parkville, Vic. 3052, Australia

ARTICLE INFO

Article history:
Received 28 February 2008
Received in revised form 27 June 2008
Accepted 27 June 2008
Available online 9 July 2008

Keywords:
Trioxolane
Iron
Quantum chemistry
Antimalarial
Density functional methods

ABSTRACT

Quantum chemical methods were used to obtain a structure for the peroxide–iron intermediate complex required for the inner-sphere reduction of dispiro-1,2,4-trioxolane antimalarials. Investigation of this biologically important interaction with iron(II) allows further understanding of the mechanisms of action and clearance of this promising new class of fully synthetic peroxide antimalarials. UHF, B3LYP and B3LYP//MP2 calculations were undertaken to provide structural and energetic information about the coordination complex of iron(II) with five representative trioxolanes, ranging in both iron-mediated reactivity and antimalarial activity. Significant energy differences were observed between the conformational isomers of these trioxolanes, indicating the importance of steric interactions between the iron complex ligands and the trioxolane substituents. These calculations may explain the slower iron-mediated reaction rates of trioxolanes that preferentially adopt a conformation that sterically shields the peroxide bond. The relationship between antimalarial activity and accessibility of the peroxide bond to iron has also been demonstrated for these trioxolanes.

1. Introduction

The current problem of multi-drug resistance to existing antimalarials has lead to a major focus on the development of new synthetic peroxide antimalarials [1]. Semi-synthetic artemisinin derivatives are currently the recommended first-line treatment for uncomplicated *Plasmodium falciparum* malaria; however to improve access to antimalarial therapy there is a need for development of synthetic peroxides at lower cost, with improved biopharmaceutical properties [2,3]. The development of the dispiro-1,2,4-trioxolanes (including OZ277; Fig. 1) is an example of the clinical potential of new fully synthetic peroxide antimalarials with excellent activity, economical synthesis and improved physicochemical and pharmacokinetic properties [4].

The mechanism of action of peroxide antimalarials involves interaction with intraparasitic iron(II), resulting in peroxide cleavage that produces the reactive species thought to mediate parasite killing [5–7]. The importance of iron for trioxolane activity has been confirmed by incubation of OZ277 (**1**) with the iron-chelating agent desferrioxamine, which antagonised *in vitro* antimalarial activity [8]. The reaction of active trioxolanes with iron(II) was found to result in the formation of potentially toxic carbon-centred free radicals, which are proposed to be responsible for antimalarial activity due to alkylation of vital parasite components [9,10]. Trioxolane reactivity with iron suggests a role for iron-containing haem, which is present at extremely high concentrations within infected erythrocytes [11]. Furthermore, iron-mediated peroxide degradation is likely to represent a significant clearance pathway for peroxide antimalarials *in vivo* [12,13].

Previous work has shown that trioxolane structure has a strong influence on iron-mediated degradation rates. The major structural influence was the steric effect of substituents around the peroxide bond, and it was suggested that this steric hindrance was related to the preferred conformation of the spirocyclohexane substituent in solution [10]. The aim of the present study was to further characterise the molecular interaction of trioxolanes with inorganic iron(II) using computational quantum chemical methods. Iron-mediated reduction of peroxides generally requires initial substitution of the peroxide into the inner coordination sphere of iron before electron transfer proceeds [14], and this intermediate trioxolane–iron complex was the focus of this study. The influence of trioxolane structure and conformation was investigated for the coordination complex of structurally representative trioxolanes with the octahedral aqueous Fe(II) ion. Quantum chemical modelling of the iron complex allows a more accurate under-

* Corresponding author. Tel.: +61 399039110.
E-mail address: david.chalmers@vcp.monash.edu.au (D.K. Chalmers).

1093-3263/$ – see front matter © 2008 Elsevier Inc. All rights reserved.
doi:10.1016/j.jmgm.2008.06.008

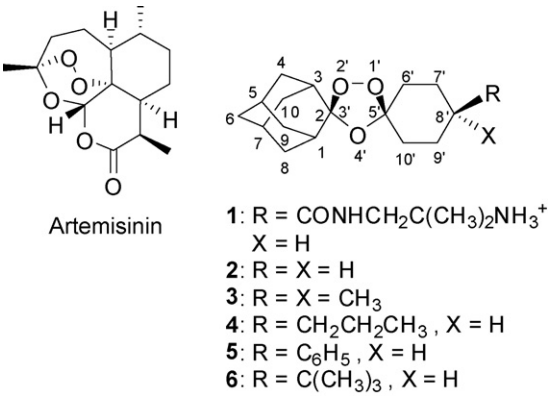

Fig. 1. Structures of artemisinin, OZ277 (**1**) and trioxolanes **2**–**6**.

standing of factors affecting the interaction with iron, compared to previous studies of the uncomplexed trioxolane structures [10,15]. The structure and minimised energies for both possible conformations of iron-complexed and uncomplexed trioxolanes are presented, and the impact on iron-mediated reaction rates and antimalarial activity is described.

After completing this study we became aware of a quantum chemical modelling study of iron bonding to artemisinin and two smaller model structures by Drew et al. [16] Their conclusion was that no intermediate trioxolane–iron complex was formed but rather the approach of a hydrated Fe(II) ion lead to immediate cleavage of the O–O bond.

2. Computational methods

Ab initio quantum chemistry calculations were performed with the 6-31G* basis set [17–20] using the Gaussian 03 program [21]. The structures of uncomplexed trioxolanes were first optimised to a local minimum at the restricted Hartree–Fock (RHF) level, which is appropriate considering the singlet state of these molecules. The stationary point was confirmed as a local minimum by showing that the Hessian had all positive eigenvalues. The structures were also optimised using the hybrid density functional theory B3LYP [22,23]. Again, the Hessian was calculated to confirm a local minimum. A single point calculation was then carried out using Møller–Plesset theory to second order (MP2//B3LYP) [24–26].

Trioxolane complexes with octahedral Fe(II) iron and five water ligands were determined with an overall charge of 2+ and high spin state, with four unpaired electrons [14]. It was confirmed using the unsubstituted 1,2,4-trioxolane ring ($C_2H_4O_3$) that this state is lower in energy (214.2 kJ/mol) than the triplet with two unpaired electrons or the singlet with no unpaired electrons (336.4 kJ/mol). Unrestricted Hartree–Fock (UHF) calculations showed that this ground state was only slightly contaminated by states of higher multiplicity with $\langle S^2 \rangle$ being between the value of 6.00 for the pure state and 6.05.

Table 1
Energy difference (kJ/mol) between conformations A and B (Fig. 2) and iron-mediated degradation rates of trioxolanes **2**–**6**

Compound	ΔE (RHF)	ΔE (B3LYP)	ΔE (MP2//B3LYP)	Fe(II) reactivity, $k \pm$ S.D. (h^{-1})[a]
2	−0.82	−1.26	0.31	0.41 ± 0.02
3	−1.01	−1.24	0.09	0.35 ± 0.02
4	−10.25	−9.49	−5.54	0.042 ± 0.002
5	−18.31	−15.19	−11.25	0.005 ± 0.001
6	−26.03	−22.73	−21.17	0.0004 ± 0.0008

$\Delta E = E_B - E_A$.
[a] Pseudo-first-order reaction rate of trioxolane (0.03 mM) with $FeSO_4$ (3 mM) in 50% ACN/H_2O at 37 °C [10].

The structures of the iron(II) complexes, coordinated to the 1′ oxygen atom of each trioxolane, were optimised using UHF and B3LYP and confirmed by calculation of the Hessians. Single point calculations at the MP2//B3LYP level of theory were also obtained. Calculations with the $[Fe(H_2O)_5]^{2+}$ group moved to the 2′ oxygen atom of the trioxolane ring of **2**, and studies of the transition structure for the movement between the 1′ and 2′ oxygen atoms, were carried out only at the UHF/6-31G* level of theory.

3. Results

3.1. Optimisation of trioxolanes 2–6

Representative trioxolanes **2**–**6** (Fig. 1), with a wide range of reported iron-mediated reaction rates [10] and antimalarial activities [27], were studied to investigate the effect of a variety of substituents at the 8′ position on structure and conformation. The cyclohexane ring of these trioxolanes may adopt one of two possible conformations, whereby the peroxide group is either in an equatorial (A) or axial (B) orientation (Fig. 2). The energies of both conformations were calculated to compare the relative thermodynamic equilibria for each trioxolane in the uncomplexed form present in solution (Table 1).

Trioxolanes **2** and **3** showed no significant preference for either conformation; however the *cis*-8′-substituted trioxolanes **4**–**6** displayed a significant preference for conformation B. This conformation allows favourable equatorial orientation of the 8′-substituent compared to the alternative axial orientation, which has increased energy due to 1,3-diaxial interactions involving the 8′-substituent. The energy differences revealed an increased preference for conformation B as the steric bulk of the *cis*-8′-substituent increased (Table 1), and were in general agreement with previous results based on molecular mechanics calculations [10].

3.2. Structure of the iron complex with trioxolanes 2–6

The proposed intermediate iron(II) complex was found for trioxolanes **2**–**6** using both UHF and B3LYP. With this clear local minimum structure for the iron complex, further investigations

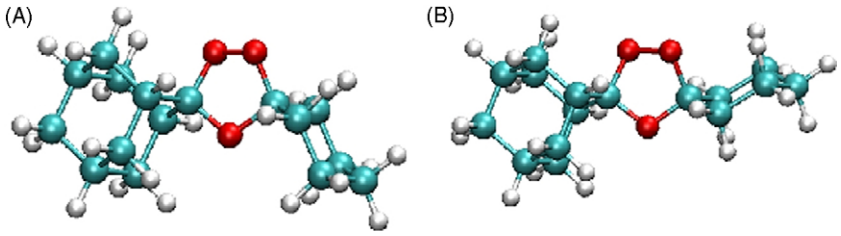

Fig. 2. Structures of trioxolane **2**, with the cyclohexane ring in either the peroxide-equatorial (A) or peroxide-axial (B) conformation.

Fig. 3. The artemisinin model compound studied by Drew et al.

were carried out to clarify why Drew et al. found no local minimum for the complex. Their approach was to use a pure DFT method, the TZP basis set and the ADF computer program. They found that the approach of $Fe(H_2O)_5$ proceeded directly to splitting of the O–O bond with generally one proton from a water molecule bonded to iron transferring to the O atom not bonding directly to the iron. We have made several studies on the smallest of the model compounds (structure **3** in [16], Fig. 3). Pure DFT methods such as BVP86, as used by Drew et al., and BLYP, with basis sets 6-31G*, TZV and TZVP, as defined in Gaussian 03, lead directly to a splitting of the O–O bond as found by Drew et al., although transfer of a proton from water to the ring breaking O atom was not observed. In contrast UHF, MP2 and the hybrid DFT methods B3LYP and B3P86 all gave a local minimum for the complex with no lengthening of the O–O bond. The structure studied here is significantly smaller than the dispiro-1,2,4-trioxolanes, allowing the more expensive MP2 method to be used with the 6-31G* basis set.

Using the open structure found with BVP86/6-31G* as a starting structure, the B3LYP/6-31G* open structure was found. This lies 22.7 kJ/mol below the complex. The transition structure between the complex and the ring-opened form was then determined and found to lie 35.8 kJ/mol above the complex. This value is slightly greater than the barrier of 25 kJ/mol found [14] for the breaking of the O–O bond in $[Fe(H_2O)^5\ (H_2O_2)]^{2+}$. Thus the barrier for reaction from the complex to the open structure is quite small.

The use of the pure DFT methods and the 6-31G* basis for the trioxolane **2**, the smallest of the test molecules studied here, also lead to direct splitting of the O–O bond without forming a stable complex. Our conclusion is that hybrid DFT, Hartree–Fock and MP2 methods give a local minimum for the complex while pure DFT methods result in direct cleavage of the peroxide bond. Hybrid DFT methods generally perform better than pure DFT methods, and as they agree also with UHF and MP2, it seems most likely that a complex is formed and then dissociates over a small barrier. This issue needs to be further studied, but as the barrier from the complex to the open structure is small, the difference between the methods is perhaps not as significant as it might appear.

The iron–peroxide complex structures for a number of 8′-substituted trioxolanes were calculated to investigate the steric effects of cyclohexane substitution. The structures of the peroxide equatorial and peroxide axial complexes are shown in Fig. 4 and energies are reported in Table 2.

For trioxolane **2**, a significant energy difference was found using all three levels of theory, indicating that conformation A is preferred to conformation B. The 8′,8′-dimethyl substituted trioxolane **3** formed complexes similar to those seen for trioxolane **2**, and conformer A was preferred over conformer B in a similar manner. This is consistent with the similar iron-mediated reaction rates observed for these compounds (Table 1).

Energy minimisation of the complex with 8′-*n*-propyl substituted trioxolane **4** revealed no significant preference for either conformation. However, taking into account the lower energy of conformation B in uncomplexed **4** (Table 1), coordination with iron increases the energy of conformation B to a greater extent than conformation A. This is in agreement with the favourable iron complexation of conformer A observed for trioxolanes **2** and **3**.

The iron complex with **5** in conformation B displayed significantly higher energy than conformation A, revealing greater interaction between the iron ligands and the phenyl substituent than was seen for the alkyl substituents. A discrepancy between MP2 and B3LYP energies was observed, and we suggest that this is due to the different handling of dispersion interactions by B3LYP and MP2 [28]. All methods showed a clear preference for conformation A.

For the iron complex of 8′-*t*-butyl substituted trioxolane **6**, the overall energy of conformation B remained much lower than conformation A, which is consistent with the much higher energy of conformation A for uncomplexed **6** (Table 1). This result indicates that the trioxolane–iron complex **6**A is not energetically favourable, which may explain the limited iron-mediated reactivity of this trioxolane.

In order to investigate the steric impact of the adamantane substituent, the peroxide–iron complex of **2**, with the iron coordinated to the O2′ atom adjacent to the adamantane moiety, was determined by UHF calculations. The total energy of this complex in conformation B was only marginally greater than for the O1′-coordinated complex (1.05 kJ/mol). The O2′-coordinated complex of conformer A was significantly higher in energy than the O1′ complex (9.04 kJ/mol), demonstrating increased steric hindrance around the adjacent peroxide oxygen afforded by the adamantane group compared to the peroxide-equatorially oriented cyclohexane ring. The steric repulsion of the adamantane substituent is further evidenced by the increased Fe–O2′ bond length (2.31 Å) compared to the O1′-coordinated complex (2.20 Å). This less favourable O2′-coordination is consistent with the selective reduction observed at the more exposed O1′ atom of these peroxides [9,10].

Furthermore, it is possible that any iron bound to the sterically congested O2′ atom may relocate to the more exposed O1′ atom before reduction of the peroxide bond occurs. The energy of the transition state for the transfer of iron from O2′ to O1′, lies only 11.30 kJ/mol higher than the O2′-coordinated complex of **2**A. This is a small barrier to a rearrangement resulting in a net energy decrease of 9.04 kJ/mol. All attempts to locate the transition structure in conformation B failed, with the iron moving to the O1′ position and the water ligands rotated by 45° to give a rotational transition structure.

Table 2
Energy difference (kJ/mol) between conformations A and B for iron(II) complexes, and antimalarial activity of trioxolanes

Compound	ΔE (UHF)	ΔE (B3LYP)	ΔE (MP2//B3LYP)	Activity[a] IC_{50} (ng/mL)
2	11.61	7.71	8.74	1.0
3	10.46	6.06	6.68	2.3
4	1.11	−2.82	0.56	1.1
5	10.05	4.60	36.84	2.2
6	−15.07	−15.57	−15.05	63

$\Delta E = E_B - E_A$.
[a] *In vitro* activity against chloroquine resistant (K1) *Plasmodium falciparum* [27].

3.3. Relationship between conformation, iron-mediated reactivity and antimalarial activity

The relative abundance of each conformation of the uncomplexed trioxolanes **2**–**6** in solution at 37 °C was estimated according to the Boltzmann distribution, using each of the three methods of energy calculation (Table 1). The percentage of trioxolane in conformation A was closely correlated to the iron-mediated reaction rates of these trioxolanes (Fig. 5A), suggesting that trioxolane reactivity is determined by the prevalence of conformer A in solution. Interestingly, there was no correlation between the preferred conformation of the iron-complexed

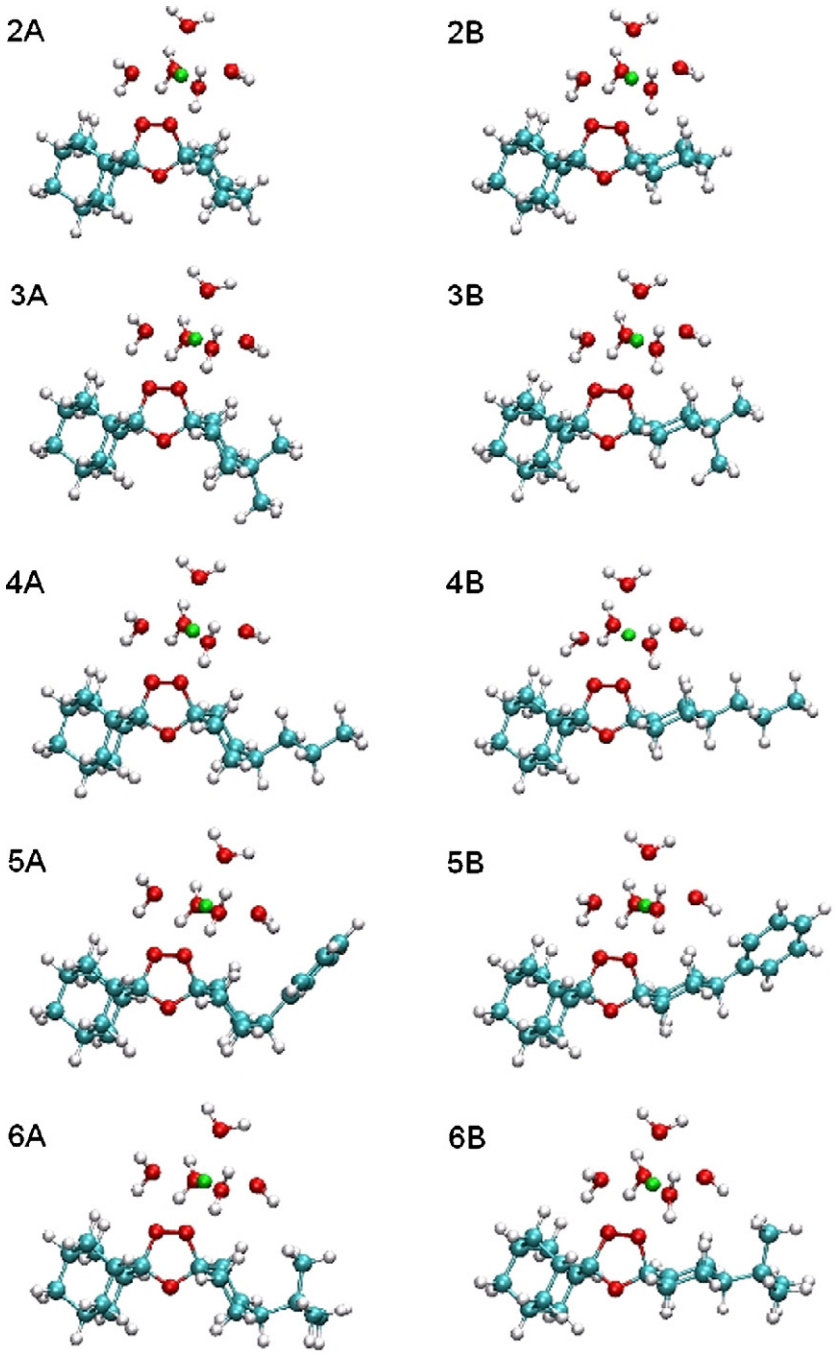

Fig. 4. Optimised structures (B3LYP) for iron(II)-complexed trioxolanes **2**–**6** in peroxide-equatorial (A) and peroxide-axial (B) conformations.

trioxolanes and iron-mediated reaction rates (Fig. 5B). A general relationship with antimalarial activity was observed, as the highly active trioxolanes **2**–**5** (Table 2) preferentially formed an iron complex in the reactive conformation A, and the poorly active (and least reactive) trioxolane **6** is unlikely to form an iron complex to any significant extent in this conformation.

4. Discussion

The structures of the complexes formed between iron(II) and various trioxolanes offer some insight into the differences in iron-mediated reactivity and antimalarial activity for these compounds. Steric interactions between iron ligands and the trioxolane substituents increase the energy of the iron–trioxolane complex, and consequently affect the reactivity with iron(II). The nature of the octahedral coordination complex of iron makes it difficult to fully model the structure of the iron complexes present in experimental measurements of chemical and biological activity. In the previous experimental studies of the iron-mediated degradation of these poorly soluble trioxolanes [9,10] the iron complex ligands are also likely to include organic solvent molecules and counter-ions, and in the biological setting a vast array of biomolecules, including the protoporphyrin of haem, is likely to coordinate the iron involved in trioxolane degradation [29]. To simplify the effects of the coordinated ligands, the calculations in this current study utilised the purely aqueous Fe(II)

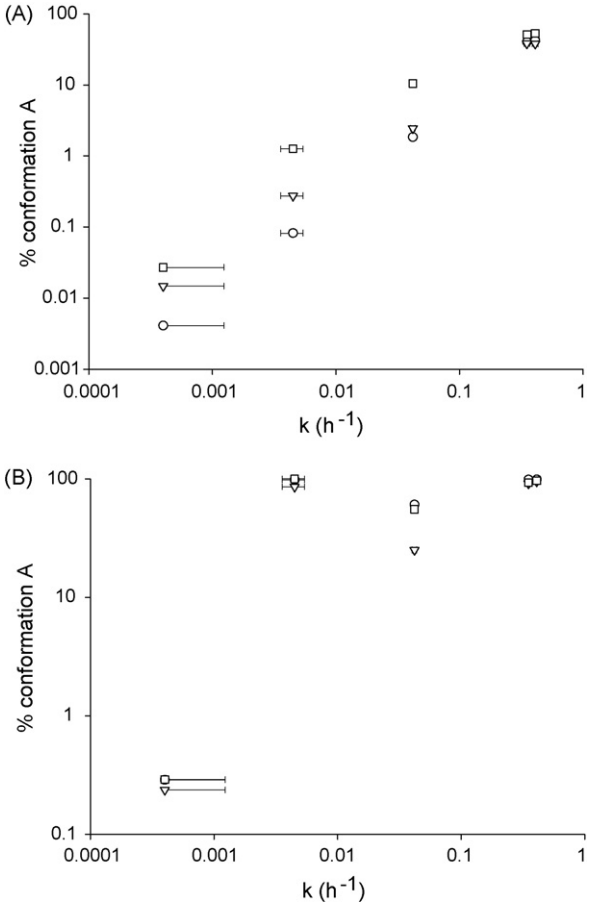

Fig. 5. Relationship between iron-mediated reaction rate ($k \pm$ S.D.) [10] and population (%) of trioxolanes in conformation A according to the Boltzmann distribution calculated at 37 °C from UHF (circles), B3LYP (triangles) and MP2//B3LYP (squares): A, uncomplexed trioxolanes; B, iron-complexed trioxolanes. (Note: iron-mediated degradation of **6** was not statistically significant and only shown here as mean + S.D. for comparison.)

complex to allow a systematic investigation of the interactions between the trioxolane substituents and the atoms coordinated to the iron centre. It should be noted that the steric interactions observed with the relatively small water ligands in this study are likely to be greater when larger coordinated ligands are involved. Furthermore, these structures indicate that the outer solvation shells of the iron complex, not studied here, are also likely to have an impact on complex formation.

The structure of the trioxolane–iron complex for **2** reveals the proximity of the cyclohexane ring to both the iron atom and the inner-sphere ligands of the iron complex. Coordination of the peroxide to iron appears feasible for both possible conformations; however the significant energy difference confers a substantial preference for conformation A. The higher energy of conformation B primarily results from greater steric interactions between the Fe(II) water ligands and the cyclohexane ring. This finding was in contrast to the suggestion by Moroni and Salvi [15] that the peroxide in conformation A would be more hindered when reacting with iron(II). The axial hydrogens (on C6′ and C10′) in conformation A are closer to the peroxide than the axial hydrogens (on C7′ and C9′) of conformer B [15]; however this current study has shown that they are actually further from the iron complex (Fig. 4). In conformer B the axial hydrogens on C7′ and C9′ are separated from the oxygens of the nearest water ligands in the iron complex by only 2.69 and 2.75 Å, which indicates very close contact, considering the combined van der Waals radii of hydrogen and oxygen is 2.72 Å [30]. In the energetically favourable conformation A these distances are almost doubled, and are not likely to contribute any significant interaction. The distances from the hydrogens on C6′ and C10′ to the nearest water ligands are shorter in conformation A (2.91 and 2.99 Å) compared to conformation B (3.46 and 3.48 Å); however this is a much smaller difference and maintains greater separation than the steric interactions at the 7′ and 9′ positions of conformer B, indicating that the peroxide is actually more exposed to attack by iron(II) when in conformation A. After superimposing the trioxolane rings of both conformers, the steric repulsion by the peroxide-axial cyclohexane conformation (2B) was confirmed by a 0.77 Å displacement of the nearest water ligand compared to the peroxide-equatorial conformation (2A). This repulsion was further confirmed by the O1′–Fe–OH_2 angle of 108° for the water ligand nearest the peroxide-axial cyclohexane ring (2B), indicating significant deviation from the octahedral angle (90°) and greater deviation (i.e. steric repulsion) than conformation A (103.9°).

Further evidence for steric inhibition imposed by the peroxide-axial cyclohexane conformation (B) is provided by the calculated energy of the complex with iron coordinated at the O2′ position. Experimentally, no significant iron-mediated reduction occurs at this oxygen adjacent to the adamantane substituent according to analysis of product formation [9,10], and the lack of reactivity of dispiroadamantane-1,2,4-trioxolane [10]. The selectivity towards reduction at the O1′ oxygen is in agreement with the greater total energy of conformer **2**A coordinated at O2′ compared to O1′. Interestingly, conformer B reveals no major difference between the total energy of the O1′ and O2′ complexes. This indicates that the steric hindrance from the peroxide-axially oriented cyclohexane group (B) is comparable to the steric hindrance from the adamantane substituent, and therefore conformer B would be unlikely to show any iron-mediated reactivity *in vitro*. These results support the hypothesis that the relatively fast iron-mediated degradation of trioxolane **2** (Table 1) is attributed to favourable coordination of iron(II) to the exposed O1′ atom of conformation A in solution.

Trioxolanes **3**–**5** also prefer iron complex formation in conformation A compared to B, due to reduced steric interactions between the cyclohexane ring and the nearest water ligand, as seen for **2**. In addition, the 8′-substituents of trioxolanes **3**–**5** may have a direct effect on the formation of the iron(II) complex, as seen by closer interactions with the complex water ligands for the higher energy B conformers compared to the A conformers. However, the impact of these substituents on the energy of complex formation is likely to be minimal, as seen by the comparable energy differences calculated for unsubstituted **2** and di-substituted **3** (Table 2). Furthermore, the similar distances between the iron complex and the 8′-substituents of **3**–**5** demonstrate that measurement of the steric proximity of these side chains cannot be used to predict iron-mediated reaction rates, which extend over two orders of magnitude for these trioxolanes. In contrast, the *t*-butyl substituent of **6** is located significantly closer to the iron complex, and this interaction may limit the iron-mediated reactivity and antimalarial activity, particularly in the presence of larger iron complex ligands and the outer coordination shell found in an experimental or biological setting.

The reaction rates for all trioxolanes in this study are primarily related to the preference of uncomplexed trioxolanes for conformation A in solution (Fig. 5). This is in agreement with studies showing faster iron-mediated reactivity [10], and lower aqueous stability [31], of trioxolanes that preferentially adopt the peroxide-equatorial cyclohexane conformation (A) due to *trans*-8′-substitution. This relationship further confirms the finding that complex formation of trioxolanes in conformation B is inhibited by

steric crowding. This inhibition of complex formation by the peroxide-axial cyclohexane may also explain the lack of iron-mediated reactivity and antimalarial activity of trioxolane **6**, which is unable to form an energetically favourable complex in the reactive conformation A.

The dependence on iron-mediated activation for the mechanism of antimalarial activity of peroxide antimalarials [5–7] highlights the need for an understanding of the factors that influence iron-mediated reactivity. This study uses a substantially improved level of theory to confirm previous assertions that steric interactions around the peroxide bond influence the interaction with iron, and therefore determine antimalarial activity. The general relationship between peroxide bond exposure, iron-mediated reactivity and antimalarial activity has also been shown for other trioxolanes [10], trioxanes [9], trioxepanes [32], tetraoxanes and hexaoxanes [33]. It therefore appears important to limit the steric hindrance around the peroxide bond when designing new synthetic peroxide antimalarials; however it is possible that excessive reactivity with iron may lead to increased drug clearance *in vivo* [10,13]. The trioxolanes in this series appear promising as they allow the iron-mediated reaction to occur in conformation A, combined with the ability to decrease the reaction rate by substitution at the 8′ position to favour conformation B.

The complex formed between iron and **4** is representative of the general peroxide–iron complex required for iron-mediated degradation of the trioxolanes (including OZ277; **1**) that have been designed to improve the pharmaceutical properties of these compounds [4,27,34,35]. It appears that modifications further along the 8′-side chains would be unlikely to interact significantly with the iron complex, but it is possible that polar or charged substituents may make favourable interactions with the complex ligands [10]. The interaction of these trioxolanes with iron *in vivo* will be additionally affected by other molecules present in the biological environment.

5. Conclusions

Calculations undertaken in this study have identified the structure of the iron–trioxolane complex involved in the iron-mediated reduction of these antimalarials. Each trioxolane in this study was found to coordinate with high-spin Fe(II) bearing five water ligands in an octahedral complex. The iron complex ligands interacted significantly with the trioxolane substituents. The adamantane moiety, and the cyclohexane ring in the peroxide-axial conformation (B), exhibited significant steric interaction with the water ligands, suggesting that iron-mediated reactivity occurs predominantly at the more exposed O1′ peroxide oxygen when the spirocyclohexane substituent is in the peroxide-equatorial conformation (A). Trioxolanes **2**–**5**, with high antimalarial activity, preferentially formed an iron complex in the peroxide-equatorial conformation (A); however poorly active **6** appears unlikely to adopt this conformation. The rate of iron-mediated trioxolane degradation was correlated with the population of peroxide-equatorial (A) conformers in solution, which can be influenced by *cis*-8′-substitution. Increasing steric bulk at the 8′-position decreases the population of peroxide-equatorial (A) conformers, thus decreasing the extent of complex formation with iron(II), resulting in slower iron-mediated degradation rates. Knowledge of the proximity of trioxolane substituents to the iron complex, and the ability of 8′-substituents to determine cyclohexane conformation, provides useful information for the future design of trioxolane antimalarials that are capable of reaction with iron, but without an excessively exposed peroxide bond that may compromise *in vivo* stability.

Acknowledgements

DJC gratefully acknowledges support provided by a Monash Silver Jubilee Postgraduate Scholarship. Computational resources were provided by the Australian Partnership for Advanced Computing National Facility.

References

[1] C.W. Jefford, New developments in synthetic peroxidic drugs as artemisinin mimics, Drug Discov. Today 12 (2007) 487–495.
[2] P.M. O'Neill, The therapeutic potential of semi-synthetic artemisinin and synthetic endoperoxide antimalarial agents, Expert Opin. Invest. Drugs 14 (2005) 1117–1128.
[3] G.A. Biagini, P.M. O'Neill, P.G. Bray, S.A. Ward, Current drug development portfolio for antimalarial therapies, Curr. Opin. Pharmacol. 5 (2005) 473–478.
[4] J.L. Vennerstrom, S. Arbe-Barnes, R. Brun, S.A. Charman, F.C.K. Chiu, J. Chollet, Y. Dong, A. Dorn, D. Hunziker, H. Matile, K. McIntosh, M. Padmanilayam, J. Santo Tomas, C. Scheurer, B. Scorneaux, Y. Tang, H. Urwyler, S. Wittlin, W.N. Charman, Identification of an antimalarial synthetic trioxolane drug development candidate, Nature 430 (2004) 900–904.
[5] Y. Dong, J.L. Vennerstrom, Mechanisms of in situ activation for peroxidic antimalarials, Redox Rep. 8 (2003) 284–288.
[6] P.M. O'Neill, G.H. Posner, A medicinal chemistry perspective on artemisinin and related endoperoxides, J. Med. Chem. 47 (2004) 2945–2964.
[7] S.R. Meshnick, Artemisinin: mechanisms of action, resistance and toxicity, Int. J. Parasitol. 32 (2002) 1655–1660.
[8] A.-C. Uhlemann, S. Wittlin, H. Matile, L.Y. Bustamante, S. Krishna, Mechanism of antimalarial action of the synthetic trioxolane RBX11160 (OZ277), Antimicrob. Agents Chemother. 51 (2007) 667–672.
[9] Y. Tang, Y. Dong, X. Wang, K. Sriraghavan, J.K. Wood, J.L. Vennerstrom, Dispiro-1,2,4-trioxane analogues of a prototype dispiro-1,2,4-trioxolane: mechanistic comparators for artemisinin in the context of reaction pathways with iron(II), J. Org. Chem. 70 (2005) 5103–5110.
[10] D.J. Creek, W.N. Charman, F.C.K. Chiu, R.J. Prankerd, K.J. McCullough, Y. Dong, J.L. Vennerstrom, S.A. Charman, Iron-mediated degradation kinetics of substituted dispiro-1,2,4-trioxolane antimalarials, J. Pharm. Sci. 96 (2007) 2945–2956.
[11] A. Robert, F. Benoit-Vical, B. Meunier, The key role of heme to trigger the antimalarial activity of trioxanes, Coord. Chem. Rev. 249 (2005) 1927–1936.
[12] L.P.D. Bishop, J.L. Maggs, P.M. O'Neill, B.K. Park, Metabolism of the antimalarial endoperoxide Ro 42-1611 (Arteflene) in the rat: evidence for endoperoxide bioactivation, J. Pharmacol. Exp. Ther. 289 (1999) 511–520.
[13] M. Padmanilayam, B. Scorneaux, Y. Dong, J. Chollet, H. Matile, S.A. Charman, D.J. Creek, W.N. Charman, J. Santo Tomas, C. Scheurer, S. Wittlin, R. Brun, J.L. Vennerstrom, Antimalarial activity of *N*-alkyl amine, carboxamide, sulfonamide, and urea derivatives of a dispiro-1,2,4-trioxolane piperidine, Bioorgan. Med. Chem. Lett. 16 (2006) 5542–5545.
[14] F. Buda, B. Ensing, M.C.M. Gribnau, E.J. Baerends, DFT study of the active intermediate in the Fenton reaction, Chem.-Eur. J. 7 (2001) 2775–2783.
[15] L. Moroni, P.R. Salvi, The structure of antimalarial dispiro-1,2,4-trioxolanes: a density functional approach, Chem. Phys. Lett. 419 (2006) 75–80.
[16] M.G.B. Drew, J. Metcalfe, F.M.D. Ismail, A DFT study of free radicals formed from artemisinin and related compounds, J. Mol. Struct. (Theochem) 711 (2004) 95–105.
[17] R. Ditchfield, W.J. Hehre, J.A. Pople, Self-consistent molecular-orbital methods. 9. Extended Gaussian-type basis for molecular-orbital studies of organic molecules, J. Chem. Phys. 54 (1971) 724–728.
[18] W.J. Hehre, R. Ditchfield, J.A. Pople, Self-consistent molecular-orbital methods. 12. Further extensions of Gaussian-type basis sets for use in molecular-orbital studies of organic-molecules, J. Chem. Phys. 56 (1972) 2257–2261.
[19] P.C. Hariharan, J.A. Pople, Influence of polarization functions on molecular-orbital hydrogenation energies, Theor. Chim. Acta 28 (1973) 213–222.
[20] V.A. Rassolov, J.A. Pople, M.A. Ratner, T.L. Windus, 6-31G* basis set for atoms K through Zn, J. Chem. Phys. 109 (1998) 1223–1229.
[21] M.J. Frisch, G.W. Trucks, H.B. Schlegel, G.E. Scuseria, M.A. Robb, J.R. Cheeseman, J.A. Montgomery Jr., T. Vreven, K.N. Kudin, J.C. Burant, J.M. Millam, S.S. Iyengar, J. Tomasi, V. Barone, B. Mennucci, M. Cossi, G. Scalmani, N. Rega, G.A. Petersson, H. Nakatsuji, M. Hada, M. Ehara, K. Toyota, R. Fukuda, J. Hasegawa, M. Ishida, T. Nakajima, Y. Honda, O. Kitao, M.H. Nakai, M. Klene, X. Li, J.E. Knox, H.P. Hratchian, J.B. Cross, V. Bakken, C. Adamo, J. Jaramillo, R. Gomperts, R.E. Stratmann, O. Yazyev, A.J. Austin, R. Cammi, C. Pomelli, J.W. Ochterski, P.Y. Ayala, K. Morokuma, G.A. Voth, J.J. Salvador, J.J. Dannenberg, V.G. Zakrzewski, S. Dapprich, A.D. Daniels, M.C. Strain, O. Farkas, D.K. Malick, A.D. Rabuck, K. Raghavachari, J.B. Foresman, J.V. Ortiz, Q. Cui, A.G. Baboul, S. Clifford, J. Cioslowski, B.B. Stefanov, G. Liu, A. Liashenko, P. Piskorz, I. Komaromi, R.L. Martin, D.J. Fox, T. Keith, M.A. Al-Laham, C.Y. Peng, A. Nanayakkara, M. Challacombe, P.M.W. Gill, B. Johnson,W. Chen, M.W. Wong, C. Gonzalez, J.A. Pople, Gaussian 03, Revision D.01, Gaussian, Inc., Wallingford, CT, 2004.
[22] A.D. Becke, Density-functional thermochemistry. 3. The role of exact exchange, J. Chem. Phys. 98 (1993) 5648–5652.
[23] P.J. Stephens, F.J. Devlin, C.F. Chabalowski, M.J. Frisch, Ab-initio calculation of vibrational absorption and circular-dichroism spectra using density-functional force-fields, J. Phys. Chem. 98 (1994) 11623–11627.

[24] M. Head-Gordon, J.A. Pople, M.J. Frisch, MP2 energy evaluation by direct methods, Chem. Phys. Lett. 153 (1988) 503–506.
[25] C. Møller, M.S. Plesset, Note on an approximation treatment for many-electron systems, Phys. Rev. 46 (1934) 0618–0622.
[26] J.A. Pople, J.S. Binkley, R. Seeger, Closed shell 2nd order Møller–Plesset and MP2 gradient, Int. J. Quantum Chem. S10 (1976) 1–19.
[27] Y. Dong, J. Chollet, H. Matile, S.A. Charman, F.C.K. Chiu, W.N. Charman, B. Scorneaux, H. Urwyler, J. Santo Tomas, C. Scheurer, C. Snyder, A. Dorn, X. Wang, J.M. Karle, Y. Tang, S. Wittlin, R. Brun, J.L. Vennerstrom, Spiro and dispiro-1,2,4-trioxolanes as antimalarial peroxides: charting a workable structure–activity relationship using simple prototypes, J. Med. Chem. 48 (2005) 4953–4961.
[28] S. Tsuzuki, H.P. Lüthi, Interaction energies of van der Waals and hydrogen bonded systems calculated using density functional theory: assessing the PW91 model, J. Chem. Phys. 114 (2001) 3949–3957.
[29] D.J. Creek, F.C.K. Chiu, R.J. Prankerd, S.A. Charman, W.N. Charman, Kinetics of iron-mediated artemisinin degradation: effect of solvent composition and iron salt, J. Pharm. Sci. 94 (2005) 1820–1829.
[30] A. Bondi, van der Waals volumes and radii, J. Phys. Chem. 68 (1964) 441–451.
[31] C. Perry, S.A. Charman, R.J. Prankerd, F.C.K. Chiu, Y. Dong, J.L. Vennerstrom, W.N. Charman, Chemical kinetics and aqueous degradation pathways of a new class of synthetic ozonide antimalarials, J. Pharm. Sci. 95 (2006) 737–747.
[32] R. Amewu, A.V. Stachulski, N.G. Berry, S.A. Ward, J. Davies, G. Labat, J.-F. Rossignol, P.M. O'Neill, Synthesis of 1,2,4-trioxepanes via application of thiol-olefin co-oxygenation methodology, Bioorgan. Med. Chem. Lett. 16 (2006) 6124–6130.
[33] Y. Dong, D. Creek, J. Chollet, H. Matile, S.A. Charman, S. Wittlin, J.K. Wood, J.L. Vennerstrom, Comparative antimalarial activities of six pairs of 1,2,4,5-tetraoxanes (peroxide dimers) and 1,2,4,5,7,8-hexaoxonanes (peroxide trimers), Antimicrob. Agents Chemother. 51 (2007) 3033–3035.
[34] Y. Dong, Y. Tang, J. Chollet, H. Matile, S. Wittlin, S.A. Charman, W.N. Charman, J. Santo Tomas, C. Scheurer, C. Snyder, B. Scorneaux, S. Bajpai, S.A. Alexander, X. Wang, M. Padmanilayam, S.R. Cheruku, R. Brun, J.L. Vennerstrom, Effect of functional group polarity on the antimalarial activity of spiro and dispiro-1,2,4-trioxolanes, Bioorg. Med. Chem. 14 (2006) 6368–6382.
[35] Y. Tang, Y. Dong, S. Wittlin, S.A. Charman, J. Chollet, F.C.K. Chiu, W.N. Charman, H. Matile, H. Urwyler, A. Dorn, S. Bajpai, X. Wang, M. Padmanilayam, J.M. Karle, R. Brun, J.L. Vennerstrom, Weak base dispiro-1,2,4-trioxolanes: potent antimalarial ozonides, Bioorgan. Med. Chem. Lett. 17 (2007) 1260–1265.